AIP | Applied Physics Letters

Single photon emission of a charge-tunable GaAs/Al0.25Ga0.75As droplet quantum dot device

Fabian Langer, David Plischke, Martin Kamp, and Sven Höfling

Citation: Applied Physics Letters **105**, 081111 (2014); doi: 10.1063/1.4894372
View online: http://dx.doi.org/10.1063/1.4894372
View Table of Contents: http://scitation.aip.org/content/aip/journal/apl/105/8?ver=pdfcov
Published by the AIP Publishing

Articles you may be interested in

Single photon emission from positioned GaAs/AlGaAs photonic nanowires
Appl. Phys. Lett. **96**, 211117 (2010); 10.1063/1.3440967

Hole recapture limited single photon generation from a single n -type charge-tunable quantum dot
Appl. Phys. Lett. **92**, 193103 (2008); 10.1063/1.2924315

Photon antibunching at high temperature from a single InGaAs/GaAs quantum dot
Appl. Phys. Lett. **84**, 1260 (2004); 10.1063/1.1650032

Temperature-dependent photoluminescence of In 0.5 Al 0.5 As/Al 0.25 Ga 0.75 As self-organized quantum dots
J. Appl. Phys. **85**, 2997 (1999); 10.1063/1.369618

APL Photonics

Reuse of AIP Publishing content is subject to the terms at: https://publishing.aip.org/authors/rights-and-permissions. IP: 138.251.162.234 On: Mon, 08 Feb 2016 10:33:44

Single photon emission of a charge-tunable GaAs/$Al_{0.25}Ga_{0.75}As$ droplet quantum dot device

Fabian Langer,[1,a)] David Plischke,[1] Martin Kamp,[1] and Sven Höfling[1,2]
[1]*Technische Physik, Physikalisches Institut and Wilhelm Conrad Röntgen Research Center for Complex Material Systems, University of Würzburg, Am Hubland, D97074 Würzburg, Germany*
[2]*SUPA, School of Physics and Astronomy, University of St Andrews, St Andrews, KY16 9SS, United Kingdom*

(Received 30 July 2014; accepted 17 August 2014; published online 28 August 2014)

In this work, we report the fabrication of a charge-tunable GaAs/$Al_{0.25}Ga_{0.75}As$ quantum dot (QD) device containing QDs deposited by modified droplet epitaxy producing almost strain and composition gradient free QDs. We obtained a QD density in the low $10^9\,cm^{-2}$ range that enables us to perform spectroscopy on single droplet QDs showing linewidths as narrow as 40 μeV. The integration of the QDs into a Schottky diode allows us to controllably charge a single QD with up to four electrons, while non-classical photoluminescence is proven by photon auto-correlation measurements showing photon-antibunching ($g^{(2)}(0) = 0.05$). © *2014 AIP Publishing LLC*.
[http://dx.doi.org/10.1063/1.4894372]

Semiconductor quantum dots (QDs) are often referred to as artificial atoms because they are characterized by a completely quantized energy-level spectrum like isolated atoms. In recent years, a number of experiments have shown the atomic-like properties of QDs, like single and entangled photon emission[1] or the shell structure of the energetic levels analogous to Hund's rule in atomic physics.[2] QDs can be made of various compounds in different material systems. Most experiments shown in the literature are performed on In(Ga)As QDs grown in Stranski-Krastanov (SK) mode on GaAs. Recently, however, modified droplet epitaxy (MDE) has emerged as a powerful alternative growth technique for producing GaAs QDs on AlGaAs.[3,4] This process creates QDs without significant material intermixing and allows to investigate all kinds of QD effects like exciton fine-structure splitting (FSS)[5] or nuclear spin dynamics[6] without the influence of strain or piezoelectric effects. Typically, MDE is performed at a low substrate temperature to form QDs in a lattice matched system causing material degeneration. A post-growth annealing process is then required to cure crystal defects. Moreover, careful calibration of the growth parameters is necessary to get low density QDs suitable for single QD spectroscopy.[7] Moreover, GaAs QDs are of interest for various devices. Recently, a QD laser containing GaAs QDs as an active medium could be shown.[8] In addition, the single photon emission of GaAs QDs has been tuned in resonance with Rb vapor around 780 nm and therewith single photons have been slowed down.[9] This makes single GaAs QDs particularly interesting for applications of hybrid atomic-QD systems for quantum technologies. Charged QDs with an excess carrier can act as quantum memories, and for this purpose it is highly important that the charging state of the QD can be well controlled.[10] But up to now, a charge-tunable GaAs/AlGaAs QD device—like it is state of the art for SK grown In(Ga)As QDs[2,11]—has not yet been demonstrated. Such a device, however, would have high scientific potential as quadrupolar interactions of the excitons with the nuclei should be significantly reduced due to the absence of strain.[12] It would, for example, be possible to use this device as a reference for all kinds of experiments in which strain between the QDs and the surrounding matrix influences interaction and decoherence phenomena. Especially, optically detected nuclear magnetic resonance could benefit as strain over the QDs reduces the sensitivity of this method drastically.[13] Although recently some ways to circumvent this limitation have emerged,[14] using a strain-free QD device is still the most straightforward way.

In this paper, we present a charge-tunable GaAs/$Al_{0.25}Ga_{0.75}As$ QD device and show charging effects of a strain free QD with up to four electrons. The sample is designed to have a low density of QDs allowing single dot spectroscopy. We made photon auto- and cross-correlation measurements to inevitably proof the QD character of the emission and to show that the photoluminescence (PL) signal from different charged states can be assigned to the same QD.

The Schottky diode containing the GaAs/$Al_{0.25}Ga_{0.75}As$ QDs was grown by solid-source molecular beam epitaxy (MBE) on GaAs(100) semi insulating substrate by MDE.[15] Ga and Al were supplied by standard effusion cells and As_2 or As_4 by a valved cracker source. After growth of the GaAs buffer layer, a 50 nm Si doped GaAs layer and a 150 nm Si doped $Al_{0.25}Ga_{0.75}As$ contact layer were deposited at a substrate temperature of 550 °C. The doping concentration in both layers was calibrated to $3 \times 10^{18}\ cm^{-3}$. Following to that and directly below the QDs a 20 nm undoped $Al_{0.25}Ga_{0.75}As$ tunnel barrier was grown. At this point, during a growth interruption, the substrate temperature was lowered to 350 °C and the As valve was closed to reduce the background As pressure. Then an amount of Ga was deposited equivalent to grow 2.26 ML of GaAs at a growth rate of 0.071 ML/s, forming Ga droplets which were crystallized in 2 min under 3×10^{-5} Torr beam equivalent pressure (BEP) of As_4. After that the substrate temperature was raised up to 400 °C and the GaAs-QDs were *in-situ* annealed for 10 min to cure crystal defects and to continue the growth of the capping layer at higher temperature.[16] Overgrowth of the QDs

a)fabian.langer@physik.uni-wuerzburg.de

 © 2014 AIP Publishing LLC

Reuse of AIP Publishing content is subject to the terms at: https://publishing.aip.org/authors/rights-and-permissions. IP: 138.251.162.234 On: Mon, 08 Feb 2016 10:33:44

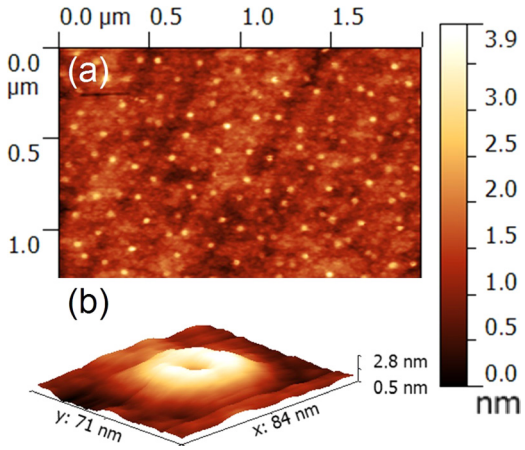

FIG. 1. AFM images taken of a sample grown to calibrate the growth parameters prior to the growth of the charge-tunable structure. (a) Detailed view of the sample surface showing a uniform formation of GaAs QDs resulting in an areal density of 5×10^9 1/cm^2. The average height of the QDs is about 3.0 nm. (b) Close up view of a single GaAs QD. The shape is ringlike with approximately 40 nm diameter.

with 10 nm $Al_{0.25}Ga_{0.75}As$ was done by migration-enhanced epitaxy (MEE).[17] Then during another growth interruption, the substrate temperature was raised back to 550 °C and 10 periods of 2 nm AlAs/2 nm $Al_{0.25}Ga_{0.75}As$ super lattice were grown to block electrons from tunneling out of the QDs when an electric field is applied. The sample was finalized by 60 nm $Al_{0.25}Ga_{0.75}As$ and a 15 nm GaAs cap.

This growth procedure leads to an areal QD density as low as 5×10^9 cm^{-2} proven by calibration samples grown before under the same conditions and measured by atomic force microscopy (AFM). A surface image of a calibration sample taken by AFM can be seen in Figure 1(a). Most of the QDs were formed with a diameter (height) of about 40 nm (3.0 nm). The achieved density is usually low enough to perform single QD experiments.[7] Moreover, one has to take into account that not all droplets are optically active. Especially, the ones with very small heights of about 1 nm are supposed to be invisible in PL measurements. The shape of the GaAs QDs was in the most cases ring like (as can be seen in Figure 1(b)) but, nevertheless, these structures show three dimensional confinement potential.[8] Before any further processing, the sample was post growth annealed for 1 min at 750 °C by rapid thermal annealing (RTA) in a nitrogen environment to cure structural crystal defects caused by the low temperature growth. These annealing conditions were found after optimization of the PL intensity and linewidths of the QD ensemble and single QD lines by both macro and micro PL measurements of differently annealed samples. To apply a vertical electric field the sample had to be prepared with ohmic contacts. Figure 2(a) shows a schematic layout of the sample after processing. At first, a 30 nm ITO layer was deposited on top of the sample by electron beam evaporation with an uncovered part left for the back contact. Then for the back contact a gold-germanium stripe was deposited on this uncovered space and alloyed at 380 °C to diffuse into the sample down to the n-doped contact layer below the QDs. After that for the top contact a gold-platinium-titanium layer was evaporated on top of the ITO layer but not alloyed this time. The processed sample was mounted on a copper heat sink and bonded with a wire bonder. Figure 2(b) shows a sketch of the conduction band edge with no bias $V_0 = 0.0$ V and with an applied forward bias of $V_1 > 0.0$ V between the two contacts. The design is comparable to the ones that have already been successfully used to charge In(Ga)As/GaAs QDs.[2,11] Under forward bias, the electronic levels of the QDs can be pushed below the Fermi level E_F and electrons can be sequentially injected from the back contact through the $Al_{0.25}Ga_{0.75}As$ tunnel barrier into the GaAs QDs. The AlAs/$Al_{0.25}Ga_{0.75}As$ super lattice prevents the charge carriers in the QDs from tunneling out of the QDs when an electric field is applied by backscattering them into the QDs.

All low-temperature, μ-PL measurements were performed using a continuous-wave 532 nm Nd:YAG laser focused by a 50× objective. The PL signal was guided into a 750 mm focal length monochromator and detected by a silicon based charge-coupled camera (CCD). The spectral resolution of the setup is well below 50 μeV. Due to the low density and the small variations in the QD sizes single QD features could be accessed.

The QD ensemble is centered around 700 nm. Most of the μPL measurements were performed in areas of low spectral density in the tails of the ensemble. The line broadenings were in the range of 50 μeV–70 μeV with some lines being as narrow as 40 μeV, what could already be lifetime limited due to the relatively thin tunnel barrier. Figure 3(a) shows a power dependent excitation series at 10 K with $V_g = 0.0$ V of

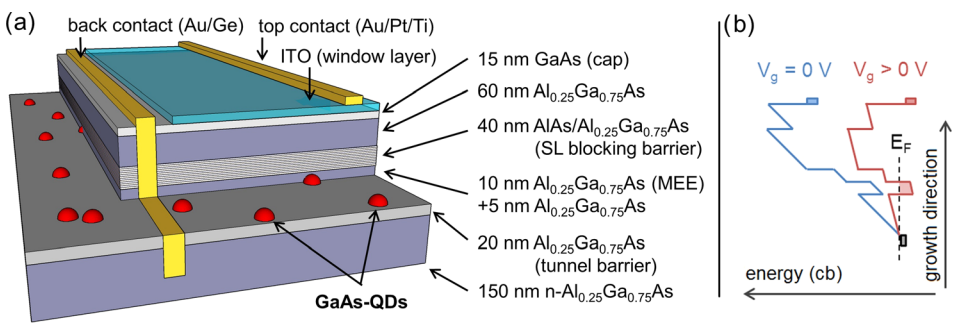

FIG. 2. (a) Schematic layout of the charge-tunable GaAs QD device. The back contact is alloyed to reach the Si doped $Al_{0.25}Ga_{0.75}As$ layer below the QDs, whereas the top contact is not. To prevent electrons in the QDs from tunneling out when an electric field is applied a short period AlAs/$Al_{0.25}Ga_{0.75}As$ super lattice acting as a blocking barrier is placed subsequent to the QD layer. (b) Schematic sketch of the conduction band edge of the charge-tunable QD device. The blue line represents the unbiased case with $V_0 = 0.0$ V, whereas the red line illustrates the conduction band level under a forward bias of $V_1 > 0.0$ V. The energetic levels of the QDs can be lowered below E_F resulting in a controlled charging of the QDs with electrons from the back contact.

Reuse of AIP Publishing content is subject to the terms at: https://publishing.aip.org/authors/rights-and-permissions. IP: 138.251.162.234 On: Mon, 08 Feb 2016 10:33:44

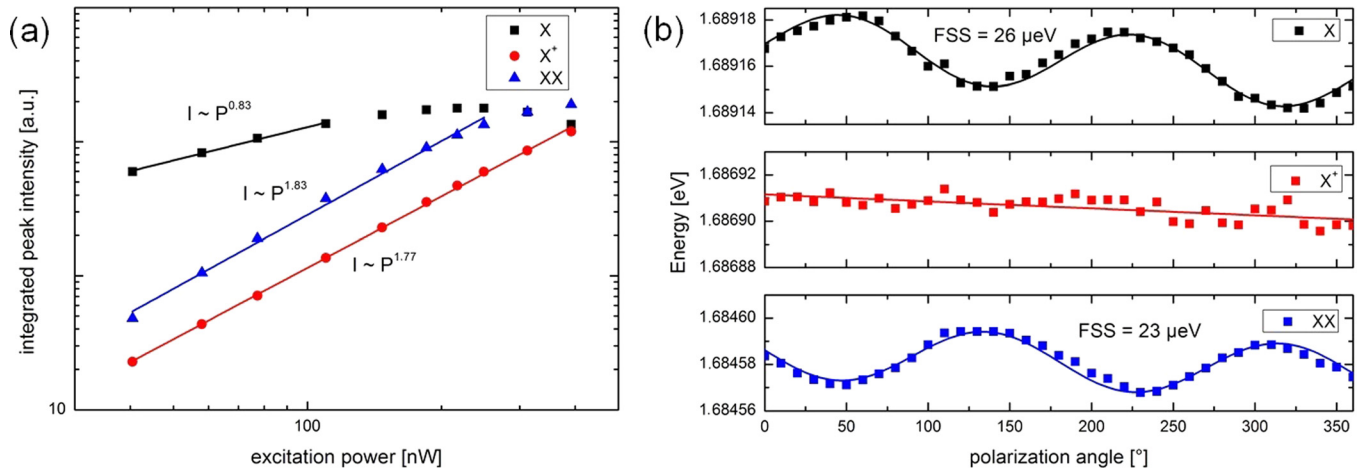

FIG. 3. μPL measurements taken at 10 K with no bias voltage applied. (a) Integrated peak intensities of three PL lines attributed to a single QD. The excitation series shows a clear excitonic-biexcitonic behavior with exponents of 0.83 for X, 1.83 for XX, and 1.77 for X^{1+}. (b) Polarization angle dependent positions of the PL lines. X and XX showing a clear sinusoidal behavior with a FSS of 26 μeV and 23 μeV, respectively, whereas for X^{1+} there is no FSS due to of the lack of electron-hole exchange interaction.

a single QD in a log-log scale. There are three PL lines visible. At low excitation power, the line with the highest intensity can be attributed to the exciton (X) what is confirmed by the exponent of the slope which shows only linear behavior with a value of 0.83. The other two lines with lower intensities can be attributed to the PL emission of the biexciton (XX) and the positively charged exciton (X^{1+}) decay. These two lines are rising with an approximately quadratic dependency with exponents of 1.83 for XX and 1.77 for X^{1+} confirming a clear exciton-biexciton behavior of the QD. In Figure 3(b), depicted is a polarization resolved series of the X, XX, and X^{1+} emission lines showing a sinusoidal behavior of X and XX as a measure of the FSS, which is 26 μeV for the exciton and 23 μeV for the biexciton. The positively charged exciton shows no FSS because of the lack of electron-hole exchange interaction.[18] The overlaying linear shift of the three emission lines is due to a small temperature instability during the measurement.

Figure 4 shows a color-scale plot of PL emission coming from a single quantum dot under an applied bias V_g ranging from 0.0 V up to 2.5 V. At a V_g of 0.3 V, there is a single sharp line representing the neutral exciton. With increasing V_g, the PL signal slowly shifts to higher energies due to the quantum confined Stark effect and suddenly jumps to somewhat lower energies at V_g of 0.55 V indicating the charging of the QD with a single electron. The difference in energy of the X and X^{1-} emission line represents the energy needed to add an electron to the neutral exciton. Besides the influence of the Stark effect the PL emission stays on the reached plateau up to 1.20 V until the electric field is strong enough to charge the QD with a second electron to form X^{2-} which again lowers the PL energy but this time much less than it was the case for the first added electron. In addition to the strong line of the X^{2-} there is a faint emission line coming up at even lower energies and staying visible for the same range of V_g. The two lines can be attributed to the splitting in singlet and triplet of the X^{2-} final state due to electron-electron interaction.[19] The bright line can be identified as the triplet state showing a fine structure splitting of 22 μeV and the faint line as the singlet state showing no fine structure splitting.[18] The clearly visible difference in PL intensity represents the three times degenerated triplet and the non degenerated singlet state. The FWHM of the lines are approximately 300 μeV for the singlet and 90 μeV for the triplet. This can be explained by the different life times of the X^{2-} final states. The singlet state can relax faster than the triplet state which needs to flip one electron spin to relax.

By further increasing V_g even higher charged states can be seen. Above 1.5 V, the PL line coming from X^{3-} becomes visible and the X^{2-} line begins to vanish and above 2.0 V the PL line from X^{4-} gets visible and the X^{3-} line starts to faint. As for X^{2-} there should also be satellite peaks for X^{3-} and X^{4-}. But due to the low PL intensity of these highly charged states, the lines are not clearly identifiable. Another interesting aspect is the tunability of the FSS with the vertical electric field. For that reason, the FSS of a neutral exciton X in dependency of the applied bias voltage V_g was estimated for three different values. We have found that the FSS could be tuned in a certain range from 36.5 μeV at $V_g = 0.35$ V to 42.5 μeV at $V_g = 0.45$ V. The tuning range is rather small due to the low confinement energies which limit the electric

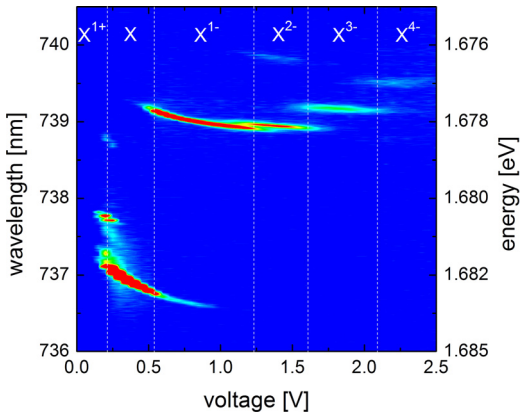

FIG. 4. Colour-scale PL plot taken at 10 K showing the charge-tunability of a single QD with up to four electrons. As the bias voltage V_g was raised from 0.0 V up to 2.5 V the PL emission abruptly jumps to distinct plateaus representing charged states of the QD. Even quantum features like the splitting into singlet and triplet state of X^{2-} can be seen.

Reuse of AIP Publishing content is subject to the terms at: https://publishing.aip.org/authors/rights-and-permissions. IP: 138.251.162.234 On: Mon, 08 Feb 2016 10:33:44

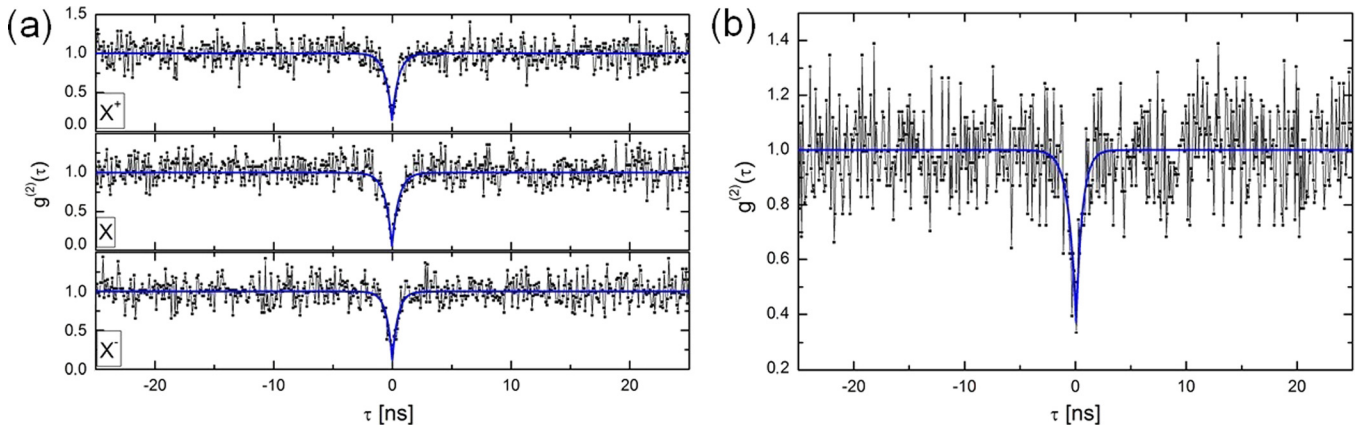

FIG. 5. (a) Photon autocorrelation measurements taken from a single QD in differently charged states showing a clear antibunching at $\tau = 0$ ns for each condition. (b) Photon cross-correlation measurements between X and X^{1-} leading to an antibunching dip at $\tau = 0$ ns.

field that can be applied until the next electron tunnels into the QD.

To further prove the quantum character of the QDs photon autocorrelation measurements were performed using a Hanbury Brown and Twiss (HBT) setup with Si-based avalanche photon diodes (APD) acting as detectors. The temporal resolution of the HBT setup was approximately 0.7 ns. The PL emission from a single QD at three different charged states was investigated at 20 K. By varying V_g, the QD could be tuned to neutral condition or charged with an electron or a hole. Figure 5(a) shows photon autocorrelation measurements of these three different states. In the histograms, a clear antibunching at $\tau = 0$ ns is visible. The data were fitted to the function

$$g^{(2)}(\tau) = 1 - (1 - g^{(2)}(0)) \exp(|\tau|/\tau_C).$$

It was then possible to obtain $g^{(2)}(0)$ and the lifetime τ_C as fit parameters. All the estimated $g^{(2)}(0)$ values are smaller than 0.5 what is known as the threshold for single photon emission. For X^{1+}, the $g^{(2)}(0)$ was 0.14 ($\pm$ 0.08), for X 0.05 ($\pm$0.05) and for X^{1-} 0.11($\pm$0.09), respectively. All of these $g^{(2)}(0)$ values are below the literature values for GaAs/AlGaAs QDs.[20,21] To finally prove that the attributed lines originate from the very same dot cross-correlation measurements were performed. Figure 5(b) shows the cross-correlation between the neutral and the negatively charged exciton. There is a clear antibunching at $\tau = 0$ ns, which this time is asymmetric: The emission of a X photon directly after the emission of an X^{1-} photon can happen very quickly because only one hole needs to be captured. For the emission of a X^{1-} photon following the emission of a X photon, however, two electrons and one hole need to be captured.[22] This takes more time resulting in the differing slopes on the two sides of the antibunching dip.

In conclusion, we have reported the growth and characterization of a charge-tunable GaAs/$Al_{0.25}Ga_{0.75}As$ QD device. A QD density being as low as 5×10^9 1/cm^2 with line broadenings down to 40 μeV could be obtained. We have been able to deterministically charge a single QD with up to four electrons and were able to observe quantum features like the non-degenerate singlet and triplet state of the X^{2-} line. The QD character of the emission was proven by photon antibunching and with cross-correlation measurements we could attribute the emissions of X and X^{1-} to a single QD. With this device, it would be possible to perform further experiments on charged QD states without the strain induced quadrupolar interaction of the excitons with the nuclei.

Technical assistance by S. Handel and M. Emmerling during sample preparation and by T. Braun during the measurements is gratefully acknowledged. Special thanks go to A. Imamoglu for stimulating discussions. This work was financially supported by the Bundesministerium für Bildung und Forschung (BMBF) within the Project "QuaHL-Rep" under Contract No. (FKZ) 01BQ1042.

[1]A. J. Shields, Nat. Photonics **1**, 215 (2007).
[2]R. J. Warburton, C. Schäflein, D. Haft, F. Bickel, A. Lorke, K. Karrai, J. M. Garcia, W. Schoenfeld, and P. M. Petroff, Nature **405**, 929 (2000).
[3]K. Watanabe, S. Tsukamoto, Y. Gotoh, and N. Koguchi, J. Cryst. Growth **227/228**, 1073 (2001).
[4]T. Mano and N. Koguchi, J. Cryst. Growth **278**, 108 (2005).
[5]M. Abbarchi, C. A. Mastrandrea, T. Kuroda, T. Mano, K. Sakoda, N. Koguchi, S. Sanguinetti, A. Vinattieri, and M. Gurioli, Phys. Rev. B **78**, 125321 (2008).
[6]T. Belhadj, T. Kuroda, C.-M. Simon, T. Amand, T. Mano, K. Sakoda, N. Koguchi, X. Marie, and B. Urbaszek, Phys. Rev. B **78**, 205325 (2008).
[7]V. Mantovani, S. Sanguinetti, M. Guzzi, E. Grilli, M. Gurioli, K. Watanabe, and N. Koguchi, J. Appl. Phys. **96**, 4416 (2004).
[8]T. Mano, T. Kuroda, K. Mitsuishi, M. Yamagiwa, X.-J. Guo, K. Furuya, K. Sakoda, and N. Koguchi, J. Cryst. Growth **301/302**, 740 (2007).
[9]N. Akopian, L. Wang, A. Rastelli, O. G. Schmidt, and V. Zwiller, Nat. Photonics **5**, 230 (2011).
[10]D. Press, K. De Greve, P. L. McMahon, T. D. Ladd, B. Friess, C. Schneider, M. Kamp, S. Höfling, A. Forchel, and Y. Yamamoto, Nat. Photonics **4**, 367 (2010).
[11]H. Drexler, D. Leonard, W. Hansen, J. P. Kotthaus, and P. M. Petroff, Phys. Rev. Lett. **73**, 2252 (1994).
[12]R. I. Dzhioev and V. L. Korenev, Phys. Rev. Lett. **99**, 037401 (2007).
[13]C. Bulutay, Phys. Rev. B **85**, 115313 (2012).
[14]E. A. Chekhovich, K. V. Kavokin, J. Puebla, A. B. Krysa, M. Hopkinson, A. D. Andreev, A. M. Sanchez, R. Beanland, M. S. Skolnick, and A. I. Tartakovskii, Nat. Nanotechnol. **7**, 646 (2012).
[15]K. Watanabe, N. Koguchi, and Y. Gotoh, Jpn. J. Appl. Phys., Part 1 **39**, L79 (2000).
[16]T. Mano, M. Abbarchi, T. Kuroda, C. A. Mastrandrea, A. Vinattieri, S. Sanguinetti, K. Sakoda, and M. Gurioli, Nanotechnology **20**, 395601 (2009).
[17]Y. Horikoshi, H. Yamaguchi, F. Briones, and M. Kawashima, J. Cryst. Growth **105**, 326 (1990).
[18]M. Bayer, A. Kuther, A. Forchel, A. Gorbunov, V. B. Timofeev, F. Schäfer, J. P. Reithmaier, T. L. Reinecke, and S. N. Walck, Phys. Rev. Lett. **82**, 1748 (1999).

Reuse of AIP Publishing content is subject to the terms at: https://publishing.aip.org/authors/rights-and-permissions. IP: 138.251.162.234 On: Mon, 08 Feb 2016 10:33:44

[19]B. Urbaszek, R. J. Warburton, K. Karrai, B. D. Gerardot, P. M. Petroff, and J. M. Garcia, Phys. Rev. Lett. **90**, 247403 (2003).
[20]M. Abbarchi, C. A. Mastrandrea, A. Vinattieri, S. Sanguinetti, T. Mano, T. Kuroda, N. Koguchi, K. Sakoda, and M. Gurioli, Phys. Rev. B **79**, 085308 (2009).
[21]T. Kuroda, M. Abbarchi, T. Mano, K. Watanabe, M. Yamagiwa, K. Kuroda, K. Sakoda, G. Kido, N. Koguchi, and C. Mastrandrea, Appl. Phys. Express **1**, 042001 (2008).
[22]M. H. Baier, A. Malko, E. Pelucchi, D. Y. Oberli, and E. Kapon, Phys. Rev. B **73**, 205321 (2006).

Reuse of AIP Publishing content is subject to the terms at: https://publishing.aip.org/authors/rights-and-permissions. IP: 138.251.162.234 On: Mon, 08 Feb 2016 10:33:44